

Article

Combining the Taguchi Method and Convolutional Neural Networks for Arrhythmia Classification by Using ECG Images with Single Heartbeats

Shu-Fen Li , Mei-Ling Huang *  and Yan-Sheng Wu

Department of Industrial Engineering & Management, National Chin-Yi University of Technology, Taichung 41170, Taiwan

* Correspondence: huangml@ncut.edu.tw

Abstract: In recent years, deep learning has been applied in numerous fields and has yielded excellent results. Convolutional neural networks (CNNs) have been used to analyze electrocardiography (ECG) data in biomedical engineering. This study combines the Taguchi method and CNNs for classifying ECG images from single heartbeats without feature extraction or signal conversion. All of the fifteen types (five classes) in the MIT-BIH Arrhythmia Dataset were included in this study. The classification accuracy achieved 96.79%, which is comparable to the state-of-the-art literature. The proposed model demonstrates effective and efficient performance in the identification of heartbeat diseases while minimizing misdiagnosis.

Keywords: Taguchi method; electrocardiography; arrhythmia; deep learning; convolutional neural network

MSC: 92C55



Citation: Li, S.-F.; Huang, M.-L.; Wu, Y.-S. Combining the Taguchi Method and Convolutional Neural Networks for Arrhythmia Classification by Using ECG Images with Single Heartbeats. *Mathematics* **2023**, *11*, 2841. <https://doi.org/10.3390/math11132841>

Academic Editor: Jakub Nalepa

Received: 28 May 2023

Revised: 18 June 2023

Accepted: 22 June 2023

Published: 24 June 2023



Copyright: © 2023 by the authors. Licensee MDPI, Basel, Switzerland. This article is an open access article distributed under the terms and conditions of the Creative Commons Attribution (CC BY) license (<https://creativecommons.org/licenses/by/4.0/>).

1. Introduction

In recent years, deep learning applications have been developed in various fields and represent effective methods to solve various identification problems [1,2]. Deep learning was first introduced by Hinton et al. and focused on automatically learning features in input data [3]. Deep learning architectures include recurrent neural networks (RNNs), long short-term memory (LSTM) networks, convolutional neural networks (CNNs), and deep belief networks (DBNs) [1,2]. Compared with conventional machine learning methods, deep learning methods exhibit superior results in the fields of image recognition [4,5], speech recognition [6], medical imaging [7–10], iris recognition [11], and face detection and recognition [12]. In the field of biomedical engineering, many scholars have started to use deep learning methods to classify lung diseases [13], diagnose breast cancer [7,14–16], recognize brain hemorrhages from computed tomography [17], and detect arrhythmia in electrocardiography (ECG) signals [18–22]. Deep learning with a CNN is prevalent and demonstrates excellent performance in speech and image recognition. Representative CNNs include LeNet [23], AlexNet [4], VGG [24], and GoogLeNet [25], which are pioneers in the field.

Most ECG-related research is based on support vector machines (SVM), the K-nearest neighbors algorithm (kNN), probabilistic neural networks (PNN), or radial basis function neural networks (RBFNN) [26–40]. The accuracy of these classification methods is 90–99%. A deep genetic ensemble of classifiers combining the advantages of ensemble learning, deep learning, and evolutionary computation was designed [41]. The computer-aided diagnosis (CAD) system of the aforementioned study was divided into four steps: (1) ECG signal preprocessing, (2) heartbeat segmentation, (3) feature extraction, and (4) classification [42]. These steps are designed to recognize heartbeat types accurately; however, these methods

are complex and cumbersome; therefore, numerous scholars have used deep learning methods in ECG in recent years [42–45]. For example, in 2016, Zubair et al. [46] used a one-dimensional (1D) CNN to classify ECG signals in the MIT-BIH Arrhythmia Database. The classification accuracy of the CNN in that study was 92.70%. In 2017, Acharya et al. [47] developed a nine-layer deep CNN to identify five categories of heartbeat automatically using ECG signals in the MIT-BIH Arrhythmia Database; this CNN's classification accuracy was 94.03%. In 2018, Oh et al. [21] proposed an automated system that used a CNN and LSTM to diagnose signals from the MIT-BIH Arrhythmia Database. The LSTM network is another widely used deep learning algorithm for analyzing time series, and the accuracy of this architecture is 98.10%. In 2018, Yildirim et al. [19] proposed the use of convolution operations in ECG; 1000 10-s ECG signal segments were used from the MIT-BIH Arrhythmia Database and classified using a 1D CNN. The overall classification accuracy was 91.33%. A novel deep learning approach for ECG heartbeat classification was conducted on the MIT-BIH Arrhythmia Database and showed more efficient results [48]. A deep residual network (ResNet) was presented for the classification of cardiac arrhythmias [49]. In 2023, a systematic review will be performed on the ECG database, preprocessing, DL methodology, evaluation paradigm, performance metric, and code availability to identify research trends, challenges, and opportunities for DL-based ECG arrhythmia classification [50].

In the aforementioned literature, CNNs have been used to detect arrhythmia in ECG signals. CNNs comprise one or more convolutional layers and a completely connected top layer (corresponding to a classical neural network); moreover, they include associated weights and a pooling layer. This structure enables CNNs to accept two-dimensional (2D) input data. CNNs provide superior results in terms of image and speech recognition compared with other deep learning structures. Moreover, CNNs can be trained using a back-propagation algorithm. Compared with other feedforward neural networks, CNNs require fewer parameters; thus, their structure is favorable for deep learning [2].

Several scholars have used 2D ECG images for analysis. In 2018, Xu et al. [10] used the modified frequency slice wavelet transform (MFSWT) on the MIT-BIH Atrial Fibrillation Database and implemented a CAD system that automatically detects atrial fibrillation. This method converts a 1-s ECG signal into a time-frequency image and then extracts and classifies the time-frequency image using a 12-layer CNN; the method achieved average accuracy, sensitivity, and specificity of 81.07%, 74.96%, and 86.41%, respectively, with five-fold cross-validation. Moreover, when unsatisfactory ECG signals were excluded from the test data, the average accuracy, sensitivity, and specificity rose to 84.85%, 79.05%, and 89.99%, respectively. The study demonstrated that atrial fibrillation could be correctly detected from transient signals. Samiee et al. [51] proposed a novel feature extraction method based on the mapping of 1D EEG signals into a 2D texture image. The fault diagnosis method first converts time-domain vibration signals into 2D gray-level images to exploit texture information from the converted images [52]. Islam et al. converted a 1D vibration signal to a 2D gray-level texture image for fault diagnosis of an induction motor [53]. Azad et al. used a multi-class support vector machine for classification on texture data of 2D images, which were transformed from 1D signals [54]. Li et al. (2018) [55] noted that although CNNs can be used to classify ECG data in the diagnosis of cardiovascular diseases, the ECG used in most related literature is a 1D ECG signal, but CNNs are more suitable for multidimensional modes or image recognition applications. The authors combined the heartbeat pattern and rhythm from 1D digital ECG signals in the MIT-BIH Arrhythmia Database and used one-hot encoding to map them onto a 2D image. Using CNN for classification, the researchers achieved an average accuracy of 99.1%. In 2018, Al Rahhal et al. [9] proposed a transfer learning method to detect and classify arrhythmia using data from the MIT-BIH Arrhythmia Database, the Institute of Cardiological Technics (INCART), and the MIT-BIH Supraventricular Arrhythmia Database (SVBD). The researchers employed a deep CNN trained on ImageNet. Since this CNN could only use images as input, they used the continuous wavelet transform (CWT) to convert 1D digital ECG signals into 2D ECG time-frequency images. The results for the MIT-BIH Arrhythmia Database, INCART, and

MIT-BIH SVDB data were superior to those obtained by previous methods. Augmented data was commonly used to provide a comprehensive understanding of the heartbeat morphology [56–59]. For example, an automated system named ‘CardioNet’ is proposed for faster and more robust classification of heartbeats for arrhythmia detection using an augmentation process [57].

The aforementioned applications of CNNs for analyzing ECG images necessitated human intervention methods (e.g., MFSWT, one-hot encoding, CWT) to convert ECG signals into images before CNN classification. This study aimed to eliminate human intervention in the ECG signal conversion process while providing satisfactory results in ECG classification. The proposed system combines the Taguchi method and CNNs for arrhythmia classification by using ECG images with single heartbeats without feature extraction or signal conversion. The main contributions of the study are as follows:

- Combining the Taguchi method and CNNs for arrhythmia classification.
- Comparing the classification results with and without electrocardiograph denoising.
- Parameter setting using orthogonal arrays in the convolution layers and max-pooling layers of the CNN.
- Successfully classifies fifteen different types of heartbeats into five major classes.
- Using ECG images with single heartbeats without feature extraction or signal conversion.

The remainder of the paper is organized as follows: The material and method, including the dataset, preprocessing, and architecture of CNN, are presented in Section 2. The experimental results, including the ECG dataset used, preprocessing, and performance using different combinations of orthogonal arrays, are given in Section 3. The comparative analysis is given in Section 4. Finally, the conclusion is drawn in Section 5.

2. Materials and Methods

2.1. Data Used

The MIT-BIH Arrhythmia Database [60] was used in this study. The database includes forty-eight 30-minute, two-lead ECG record segments comprising 15 beat types. This study divided these 15 beat types into one of the following five categories according to the Association for the Advancement of Medical Instrumentation (AAMI) EC57:1998 standard [61]: non-ectopic beats (N), supraventricular ectopic beats (S), ventricular ectopic beats (V), fusion beats (F), and unknown beats (Q). Table 1 shows the beat types in the arrhythmia database. These five categories were used for the experiments in this study.

Table 1. MIT-BIH Arrhythmia Database beat types classified according to the AAMI EC57:1998 standard.

Class	Non Ectopic Beat (N)	Supra-Ventricular Ectopic Beats (S)	Ventricular Ectopic Beats (V)	Fusion Beat (F)	Unknown Beat (Q)
Type	1. Normal beat	1. Atrial premature beat	1. Premature ventricular contraction beat	1. Fusion of ventricular and normal beat	1. Paced beat
	2. Left bundle branch block beat	2. Aberrated atrial premature beat	2. Ventricular escape beat		2. Fusion of paced and normal beats
	3. Right bundle branch block beat	3. Nodal (junctional) premature beat			3. Unclassifiable beat
	4. Atrial escape beat	4. Supra-ventricular premature beat			
	5. Nodal (junctional) escape beat				

2.2. Preprocessing

2.2.1. Electrocardiograph Denoising

When collecting ECG signals, the ECG signal amplitude can be inconsistent because of the collection instruments chosen as well as patient and environmental factors; thus, ECG signals often contain noise. However, ECG signal denoising can mostly restore the original signal.

The denoising methods for ECG signals are many. This study referred to Singh et al. [62] to select mother wavelet basis functions. Their method is mainly used to eliminate the noise superimposed on an ECG signal. Therefore, in this study, all ECG signals were denoised using a Daubechies wavelet (db8). Moreover, this study established sets of ECG images both with and without denoising to compare the classification results and determine the effect of denoising.

2.2.2. Heartbeat Segmentation

Each patient has a unique heartbeat pattern; however, in heartbeat segmentation, a separate ECG signal is formed of PQRST for a single heartbeat. Related studies using a fixed sample centered on the R peak have not ensured that a single ECG signal could contain PQRST for a single heartbeat. Therefore, this study used Equations (1) and (2) to segment heartbeats [63].

$$N_{\text{Left}} = (R_N - R_{N-1})/2 \tag{1}$$

$$N_{\text{Right}} = (R_{N+1} - R_N)/2 \tag{2}$$

$$N = N_{\text{Left}} + N_{\text{Right}} \tag{3}$$

where R_N is the position of the N th R peak, N_{Left} is the total number of samples between the $(N - 1)$ th and N th R peaks divided by 2, N_{Right} is the total number of samples between the N th and $(N + 1)$ th R peaks divided by 2, and N is the number of samples for the length of the ECG signal. Figure 1 shows a schematic of heartbeat segmentation.

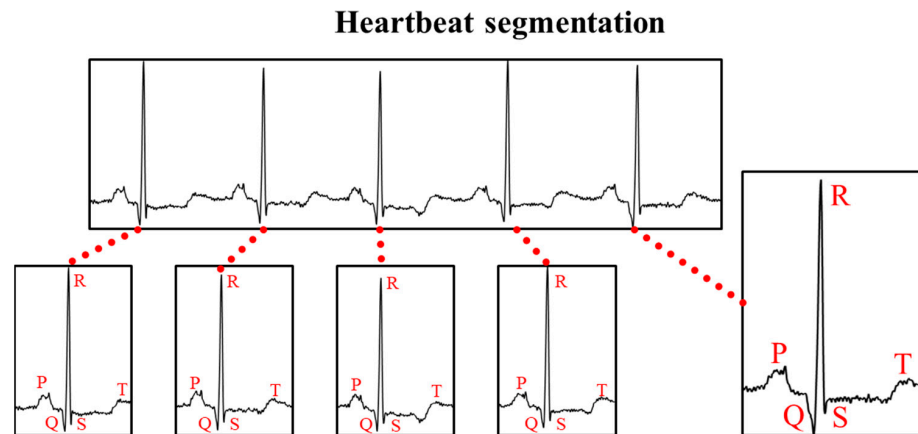


Figure 1. Schematic of heartbeat segmentation (The P wave in an ECG complex indicates atrial depolarization. The QRS is responsible for ventricular depolarization and the T wave is ventricular repolarization.).

2.3. Creating an Image Dataset

ECG signals were converted into ECG images to create an image database. MF-SWT [10], one-hot encoding [38], and CWT [9] are commonly used to draw ECG images. MFSWT and CWT map ECG signals onto spectrograms for analysis. One-hot encoding obtains ECG images by encoding ECG signal records. All of these methods use ECG signals to present ECG images in another form; thus, the original ECG signals cannot be presented. The image indicates the ECG value of the ECG signal in the corresponding time space by representing the amplitudes of the EEG signals as a function of time. Therefore, this

study plotted ECG images using preprocessed ECG signals (Figure 2). This method directly draws ECG images to obtain ECG image datasets with and without denoising.

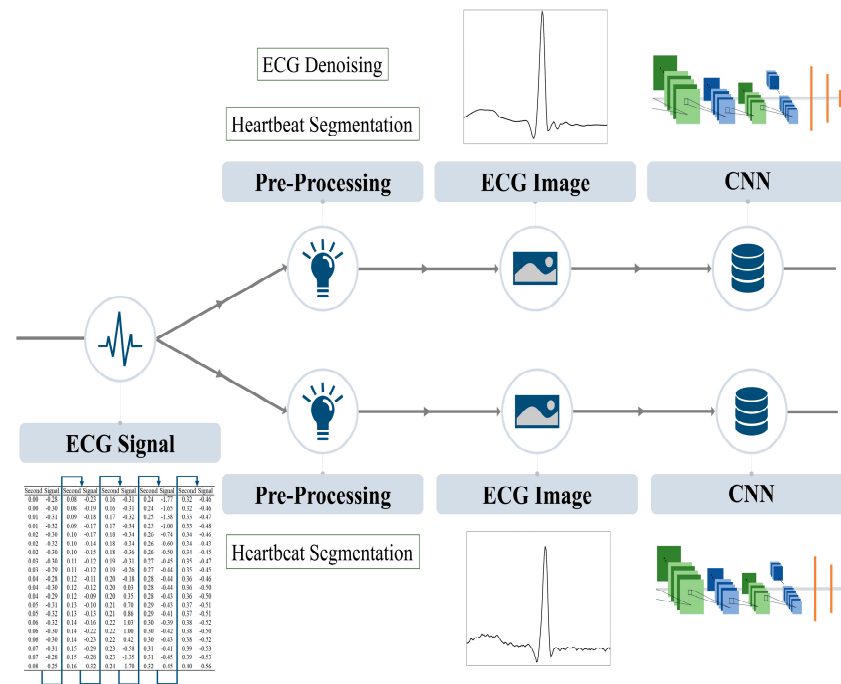


Figure 2. ECG segments for MIT-BIH Arrhythmia Database beats.

2.4. Convolutional Neural Network

A CNN is a conventional deep learning model comprising one or more convolution layers and a completely connected layer, with an image input layer, pooling layer, average pooling layer, rectified linear unit (ReLU) layer, dropout layer, and softmax layer. This architecture enables CNNs to provide superior image and speech recognition compared with other deep learning architectures [4,23–25]. This study employed a CNN because this network does not require additional methods for artificial feature extraction or classification [26–30]. The following provides a detailed description of the architecture. The more network layers, the better the learning results. However, increasing the number of network layers increases the calculation time; thus, the performance of learning architectures depends on the complexity of the problem [64]. The number of parameter combinations in CNN could be high; this study arranged CNN parameter combinations and selected the optimal configuration using a Taguchi orthogonal array. The Taguchi method identifies key effective parameters with much fewer experiments. The CNN model in the Deep Learning Library constructed in Matlab software version R2019a was used for CNN model building and execution in this study. The specification of the computer used for the calculation in this study is an Intel(R) Core(TM) i7-8700 CPU at 3.20 GHz and 3.19 GHz with a RAM of 32.0 GB.

2.4.1. Image Input Layer

The image input layer is the first layer of a CNN and is a requirement of all networks. Images with a size of 250 × 250 pixels were imported in this study.

2.4.2. Convolution Layers

A convolution is a linear operation that involves the multiplication between an array of input data and a kernel, a two-dimensional array of weights. Convolution uses a ‘kernel’ to extract certain ‘features’ from an input image. After convolution, features are generated and used as input to the subsequent layer. This study employed two convolution layers in its CNN ReLU layers.

ReLU refers to Rectified Linear Uni and is the most commonly used activation function for the outputs of the CNN neurons [65]. The function of a ReLU layer is to convert input neurons into new neuron outputs using Equation (4). In this function, x is the input of the neuron. If x is greater than 0, $h(x)$ directly outputs the input x . If x is less than or equal to 0, the output of $h(x)$ is 0. Therefore, the problem of gradient disappearance can be effectively overcome. In this study, two ReLU layers were employed after the convolution layers.

$$h(x) = \begin{cases} x(x > 0) \\ 0(x \leq 0) \end{cases} \tag{4}$$

2.4.3. Max-Pooling Layers

The pooling layers compute the maximum or average over a region of a feature map. The primary function of pooling is to reduce the number of features and parameters. Mean pooling and maximum pooling are generally used. The maximum pooling used in this study is based on the parameters of the kernel and stride set by the user to maximize adjacent feature points. This study’s CNN included two pooling layers.

2.4.4. Fully Connected Layers

The fully connected layer connects with the output of the previous layer and is typically used in the last stages of the CNN to connect to the output layer and construct the desired number of outputs. The number of outputs can be determined, and the number of categories for final classification is set or mapped to the final layer. This study utilized two fully connected layers.

2.4.5. Softmax Layer

The Softmax layer is placed just before the output layer. Softmax assumes that each example is a member of exactly one class. The Softmax layer must have the same number of nodes as the output layer. Softmax assigns decimal probabilities to each class in a multi-class problem. A softmax layer normalizes an input value to provide an output value of 0–1 using the softmax function and classifies the output according to the output value. This study employed one softmax layer in its CNN.

Table 2 details the specifics of each parameter. Conv 1 kernel size = 11×11 , 15×15 and 20×20 ; Conv 1 Number of kernel = 48 and 96; Conv 1 Stride = 4, 6 and 8; Conv 1 Padding = 1 and 2; Pooling 1 Kernel size = 3×3 and 5×5 ; Pooling 1 Stride = 2 and 3; Conv 2 kernel size = 5×5 and 7×7 ; Conv 2 Number of kernel = 128 and 256; Conv 2 Stride = 1 and 2; Conv 2 Padding = 2, 3 and 4; Pooling 2 Kernel size = 2×2 and 3×3 ; Pooling 2 Stride = 2 and 3. There are nine two-level factors and three three-level factors in total for the above twelve parameters. Dropout: randomly dropping out nodes during training was used to reduce overfitting and improve generalization error in CNN in this study. The setting of dropout was suggested from related literature. A value of 0.5 was selected for dropout from the tests of our experiments.

Table 2. Details of parameters of each layer of the proposed CNN.

No	Layer Name	Layer Parameters	Experiment
1	Image Input	Image size	250×250
2	Convolution 1	Kernel size	$11 \times 11, 15 \times 15, 20 \times 20$
		Number of Kernel	48, 96
		Stride	4, 6, 8
		Padding	1, 2
3	Activation function	ReLU	
4	Pooling 1	Kernel size	$3 \times 3, 5 \times 5$
		Stride	2, 3

Table 2. Cont.

No	Layer Name	Layer Parameters	Experiment
5	Convolution 2	Kernel size	$5 \times 5, 7 \times 7$
		Number of Kernel	128, 256
		Stride	1, 2
		Padding	2, 3, 4
6	Activation function	ReLU	
7	Pooling 2	Kernel size	$2 \times 2, 3 \times 3$
		Stride	2, 3
8	Fully Connected		1000
9	Activation function	ReLU	
10	Dropout		0.5
11	Fully Connected		5
12	Soft-max		

3. Results

3.1. Preprocessing

3.1.1. ECG Denoising

This study used a Daubechies wavelet (db8) [65] to perform denoising in MATLAB of all ECG signals in the arrhythmia database. Figure 3 shows the signal denoising results for the five categories: nonectopic beats (N), supraventricular ectopic beats (S), ventricular ectopic beats (V), fusion beats (F), and unknown beats (Q). In Figure 3, the red is the denoised signal, and the blue is the original signal. The results show that denoising can substantially reduce the noise of an ECG signal while retaining the original peak.

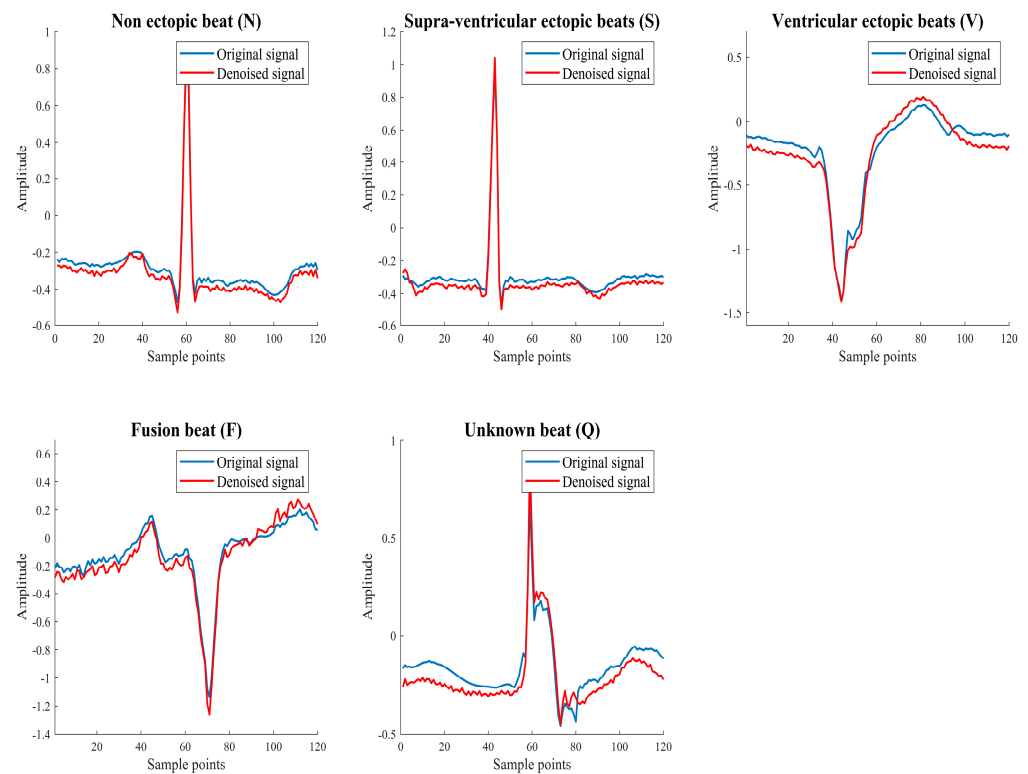


Figure 3. Denoising of MIT-BIH Arrhythmia Database recordings.

3.1.2. Heartbeat Segmentation

Table 3 shows that the heart rate of each patient is different, and thus, using a fixed time interval or a fixed number of samples to perform heartbeat segmentation would be inappropriate. Moreover, for any one patient, the heart rate may not be constant. Therefore, this study used Equations (1)–(3) to perform heartbeat segmentation for each patient, and the results are presented in Figure 4. The figure illustrates the 11–15th heartbeats of patient 100. Each patient’s heart rate was different; therefore, the number of heartbeat samples varied by patient. The resampling technique was used to ensure the input dimension of the image was the same size. Heartbeat segmentation was performed on 48 ECG signals from the MIT-BIH Arrhythmia Database; Table 1 defines the five categories based on the AAMI standard [61]. Non-ectopic beats (N) included the normal beat, left bundle branch block beat, right bundle branch block beat, atrial escape beat, and nodal escape beat. Since this type of beat accounted for 83% ($n = 90,631$) of the total heartbeats, ten percent ($90,631 \times 10\% = 9063$) non-ectopic beats were randomly selected (Table 4) in this study. Table 4 presents the number of ECG images ($N = 9063$, $S = 2781$, $V = 7236$, $F = 803$, and $Q = 8043$); 80%, 10%, and 10% of the data comprised the training, validation, and test sets, respectively, with 10-fold cross validations. Since the number of heart beats for type F was notably lower than the other four types, the succeeding experiments were split into classifying five types and four types (without type F) to compare the difference in classification performance of unbalanced data.

Through preprocessing, 27,926 ECG signals for each of two experiments—with (Experiment 1) and without (Experiment 2) denoising—were obtained, and corresponding ECG images were drawn. The size of each ECG image was 250×250 pixels.

Table 3. Heart rates of patients from the MIT-BIH Arrhythmia Database.

No.	Record	Heart Rate	No.	Record	Heart Rate	No.	Record	Heart Rate
1	100	76	21	122	83	41	222	88
2	101	62	22	123	51	42	223	88
3	102	73	23	124	54	43	228	71
4	103	70	24	200	93	44	230	82
5	104	77	25	201	68	45	231	67
6	105	90	26	202	72	46	232	61
7	106	70	27	203	104	47	233	105
8	107	71	28	205	89	48	234	92
9	108	61	29	207	80			
10	109	85	30	208	101			
11	111	71	31	209	102			
12	112	85	32	210	90			
13	113	60	33	212	92			
14	114	63	34	213	110			
15	115	65	35	214	77			
16	116	81	36	215	113			
17	117	51	37	217	76			
18	118	77	38	219	77			
19	119	70	39	220	69			
20	121	63	40	221	82			

Table 4. Number of beats by type.

Class	N	S	V	F	Q	Total
Experiment 1	9063	2781	7236	803	8043	27,926
Experiment 2	9063	2781	7236	803	8043	27,926

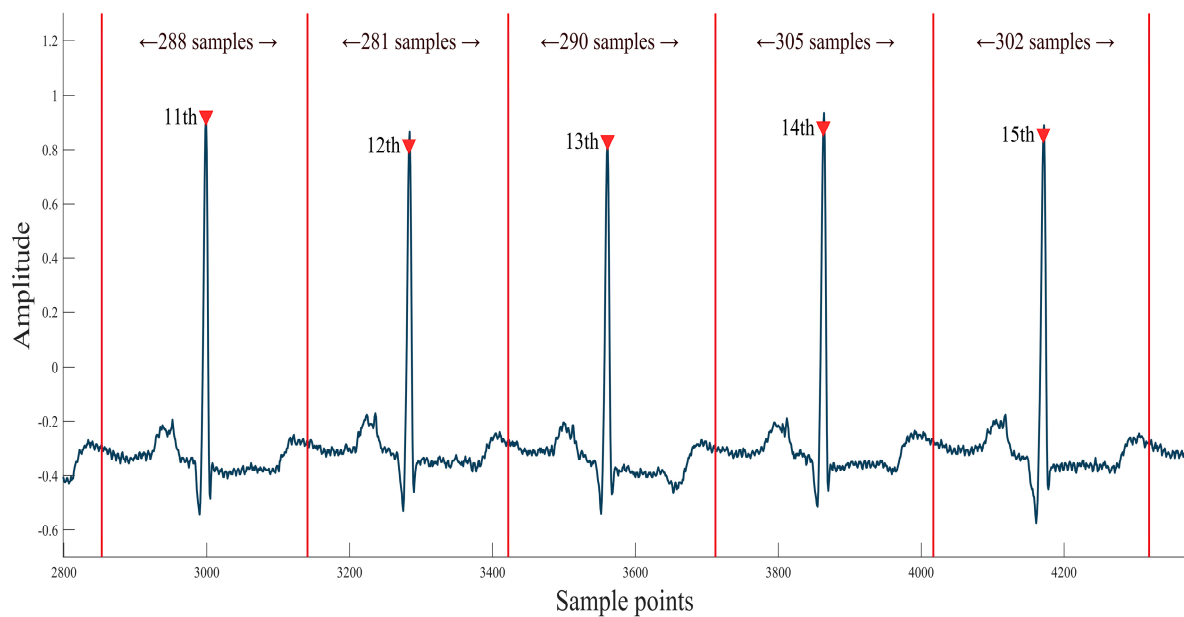


Figure 4. Heartbeat segmentation.

3.2. Convolutional Neural Network

According to Taguchi's catalog of orthogonal arrays, this study used a L_{36} orthogonal array for the parameter setting of 12 parameters (nine two-level factors and three three-level factors in Table 2) in the convolution layers and max-pooling layers of the CNN. The parameter settings are listed in Table 5. Table 5 also shows the average accuracies of CNN classification for each parameter setting in Experiments 1 and 2, which were repeated five times for the test dataset. The highest accuracy for Experiment 1 was 96.47%, and the training time was 322 s (Experiment #10). The highest accuracy for Experiment 2 was 96.79%, and the training time was 290 s (Experiment #21). The parameter values of Combination #10 for experiment 1 are Conv 1 kernel size = 11×11 , Conv 1 Number of kernel = 96, Conv 1 Stride = 4, Conv 1 Padding = 2, Pooling 1 Kernel size = 5×5 , Pooling 1 Stride = 2, Conv 2 kernel size = 7×7 , Conv 2 Number of kernel = 256, Conv 2 Stride = 1, Conv 2 Padding = 4, Pooling 2 Kernel size = 2×2 , Pooling 2 Stride = 2; the parameter values of Combination #21 for experiment 2 are: Conv 1 kernel size = 20×20 , Conv 1 Number of kernel = 48, Conv 1 Stride = 4, Conv 1 Padding = 2, Pooling 1 Kernel size = 3×3 , Pooling 1 Stride = 2, Conv 2 kernel size = 7×7 , Conv 2 Number of kernel = 256, Conv 2 Stride = 1, Conv 2 Padding = 4, Pooling 2 Kernel size = 3×3 , Pooling 2 Stride = 3. Furthermore, results showed that a smaller stride in the convolution layers corresponded to higher accuracy. This observation indicates that a smaller stride in convolution extracts more details from ECG images.

Table 5. Performance of CNN under different parameter settings.

No.	A	B	C	D	E	F	G	H	I	J	K	L	Experiment 1		Experiment 2	
	Conv1 Kernel Size	Conv1 Number of Kernel	Conv1 Stride	Conv1 Padding	Pooling 1 Kernel Size	Pooling 1 Stride	Conv2 Kernel Size	Conv2 Number of Kernel	Conv2 Stride	Conv2 Padding	Pooling 2 Kernel Size	Pooling 2 Stride	Acc.	Time Elapsed	Acc.	Time Elapsed
1	11 × 11	48	4	1	3 × 3	2	5 × 5	128	1	2	2 × 2	2	96.47%	222	96.63%	216
2	15 × 15	48	6	1	3 × 3	2	5 × 5	128	1	3	2 × 2	2	96.17%	161	96.38%	161
3	20 × 20	48	8	1	3 × 3	2	5 × 5	128	1	4	2 × 2	2	96.02%	161	96.30%	161
4	11 × 11	48	4	1	3 × 3	3	7 × 7	256	2	2	2 × 2	2	95.77%	173	95.90%	173
5	15 × 15	48	6	1	3 × 3	3	7 × 7	256	2	3	2 × 2	2	95.48%	162	95.89%	161
6	20 × 20	48	8	1	3 × 3	3	7 × 7	256	2	4	2 × 2	2	95.72%	159	95.96%	159
7	11 × 11	48	4	2	5 × 5	2	5 × 5	128	2	3	3 × 3	2	95.38%	185	95.36%	185
8	15 × 15	48	6	2	5 × 5	2	5 × 5	128	2	4	3 × 3	2	94.12%	158	94.11%	160
9	20 × 20	48	8	2	5 × 5	2	5 × 5	128	2	2	3 × 3	2	90.37%	150	92.11%	152
10	11 × 11	96	4	2	5 × 5	2	7 × 7	256	1	4	2 × 2	2	96.47%	322	96.61%	322
11	15 × 15	96	6	2	5 × 5	2	7 × 7	256	1	2	2 × 2	2	95.76%	187	96.23%	188
12	20 × 20	96	8	2	5 × 5	2	7 × 7	256	1	3	2 × 2	2	94.75%	200	95.06%	201
13	11 × 11	96	6	1	5 × 5	3	5 × 5	256	1	4	3 × 3	2	96.07%	196	95.93%	195
14	15 × 15	96	8	1	5 × 5	3	5 × 5	256	1	2	3 × 3	2	94.29%	169	94.77%	172
15	20 × 20	96	4	1	5 × 5	3	5 × 5	256	1	3	3 × 3	2	96.26%	706	96.57%	711
16	11 × 11	96	6	2	3 × 3	3	7 × 7	128	2	4	3 × 3	2	93.79%	174	93.90%	182
17	15 × 15	96	8	2	3 × 3	3	7 × 7	128	2	2	3 × 3	2	93.07%	352	93.38%	181
18	20 × 20	96	4	2	3 × 3	3	7 × 7	128	2	3	3 × 3	2	93.42%	584	93.47%	540
19	11 × 11	48	6	2	3 × 3	2	7 × 7	256	1	2	3 × 3	3	95.84%	336	96.09%	403
20	15 × 15	48	8	2	3 × 3	2	7 × 7	256	1	3	3 × 3	3	95.26%	233	95.35%	262
21	20 × 20	48	4	2	3 × 3	2	7 × 7	256	1	4	3 × 3	3	96.47%	284	96.79%	290
22	11 × 11	48	6	1	5 × 5	3	7 × 7	128	1	3	3 × 3	3	93.17%	278	93.57%	166
23	15 × 15	48	8	1	5 × 5	3	7 × 7	128	1	4	3 × 3	3	93.04%	270	93.24%	158
24	20 × 20	48	4	1	5 × 5	3	7 × 7	128	1	2	3 × 3	3	93.24%	225	93.23%	185
25	11 × 11	48	8	2	5 × 5	3	5 × 5	256	2	3	2 × 2	3	94.60%	171	94.75%	151
26	15 × 15	48	4	2	5 × 5	3	5 × 5	256	2	4	2 × 2	3	95.91%	325	96.22%	185
27	20 × 20	48	6	2	5 × 5	3	5 × 5	256	2	2	2 × 2	3	94.36%	249	94.51%	168
28	11 × 11	96	8	1	3 × 3	2	5 × 5	256	2	3	3 × 3	3	95.10%	189	95.41%	168
29	15 × 15	96	4	1	3 × 3	2	5 × 5	256	2	4	3 × 3	3	96.06%	256	96.41%	247
30	20 × 20	96	6	1	3 × 3	2	5 × 5	256	2	2	3 × 3	3	94.79%	194	94.93%	196

Table 5. Cont.

No.	A	B	C	D	E	F	G	H	I	J	K	L	Experiment 1		Experiment 2	
	Conv1 Kernel Size	Conv1 Number of Kernel	Conv1 Stride	Conv1 Padding	Pooling 1 Kernel Size	Pooling 1 Stride	Conv2 Kernel Size	Conv2 Number of Kernel	Conv2 Stride	Conv2 Padding	Pooling 2 Kernel Size	Pooling 2 Stride	Acc.	Time Elapsed	Acc.	Time Elapsed
31	11 × 11	96	8	2	3 × 3	3	5 × 5	128	1	4	2 × 2	3	95.20%	165	95.41%	173
32	15 × 15	96	4	2	3 × 3	3	5 × 5	128	1	2	2 × 2	3	95.86%	195	96.10%	204
33	20 × 20	96	6	2	3 × 3	3	5 × 5	128	1	3	2 × 2	3	95.24%	186	95.45%	195
34	11 × 11	96	8	1	5 × 5	2	7 × 7	128	2	2	2 × 2	3	91.83%	158	91.96%	254
35	15 × 15	96	4	1	5 × 5	2	7 × 7	128	2	3	2 × 2	3	95.03%	217	95.09%	498
36	20 × 20	96	6	1	5 × 5	2	7 × 7	128	2	4	2 × 2	3	92.73%	187	92.13%	321

The CNN results under each parameter setting are discussed as follows: The detailed information about the structures of the proposed CNN method that achieves the highest accuracy for Experiments 1 and 2 is shown in Figure 5. Figure 6 represents the highest accuracies of Experiments 1 and 2. Obviously, the accuracy for fusion beats (F) was considerably lower than that for the other four categories. Therefore, this study removed the F type and used CNN to classify it under the optimal parameter settings of Experiments 1 and 2. The metrics showing accuracy, precision, recall, and F1-score are listed in Table 6. For five-class classification, the accuracy, precision, recall, and F1-score for Experiment 1 are 96.47%, 95.11%, 93.27%, and 94.14%, respectively. The accuracy, precision, recall, and F1-score for Experiment 2 are 96.79%, 96.12%, 93.19%, and 94.52%, respectively. After deleting fusion beats (F), the accuracy, precision, recall, and F1-score for Experiment 1 are 97.31%, 96.80%, 96.41%, and 96.60%, respectively. The accuracy, precision, recall, and F1-score for Experiment 2 are 97.20%, 96.73%, 96.31%, and 96.51%, respectively. Figure 7 reveals that removing F did not notably improve overall accuracy because the results for each category remained similar. Thus, the results were classified into five categories. Moreover, Figure 6 reveals no substantial difference in the individual or overall classification results of Experiments 1 and 2; thus, the denoising of ECG images did not considerably improve the accuracy of classification.

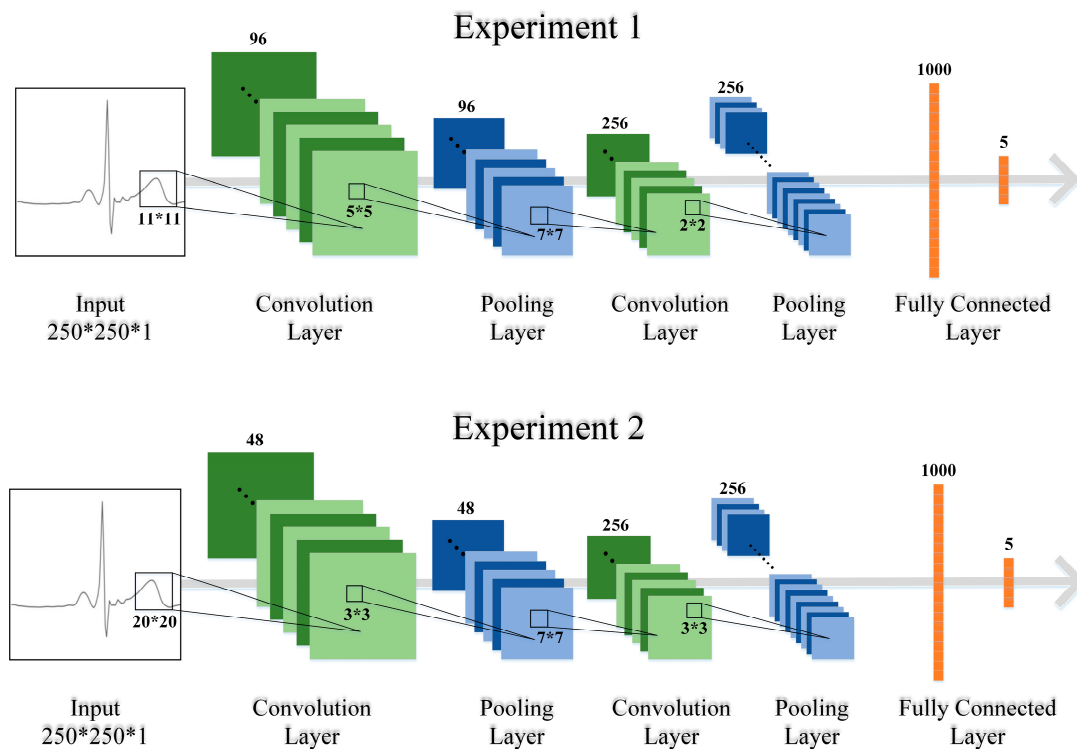


Figure 5. CNN architecture.

Table 6. Performance metrics of experiments.

	Class	Accuracy	Precision	Recall	F1-Score
Experiment 1	5	96.47%	95.11%	93.27%	94.14%
Experiment 2	5	96.79%	96.12%	93.19%	94.52%
Experiment 1	4	97.31%	96.80%	96.41%	96.60%
Experiment 2	4	97.20%	96.73%	96.31%	96.51%

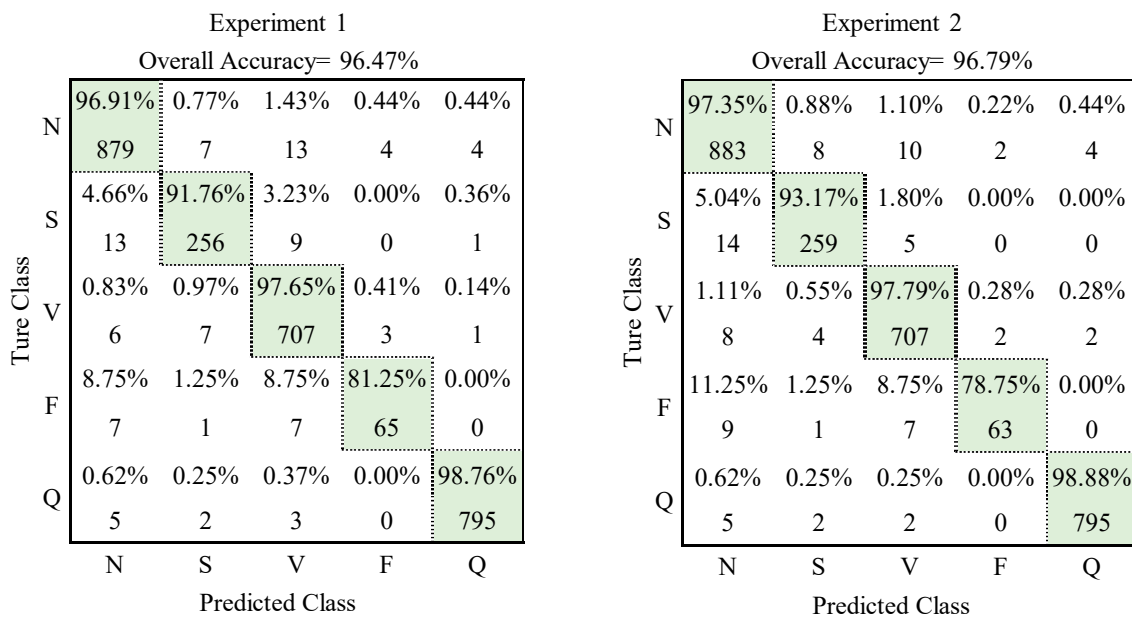


Figure 6. Experiment 1 and Experiment 2 confusion matrices of heartbeat classification results for the test data.

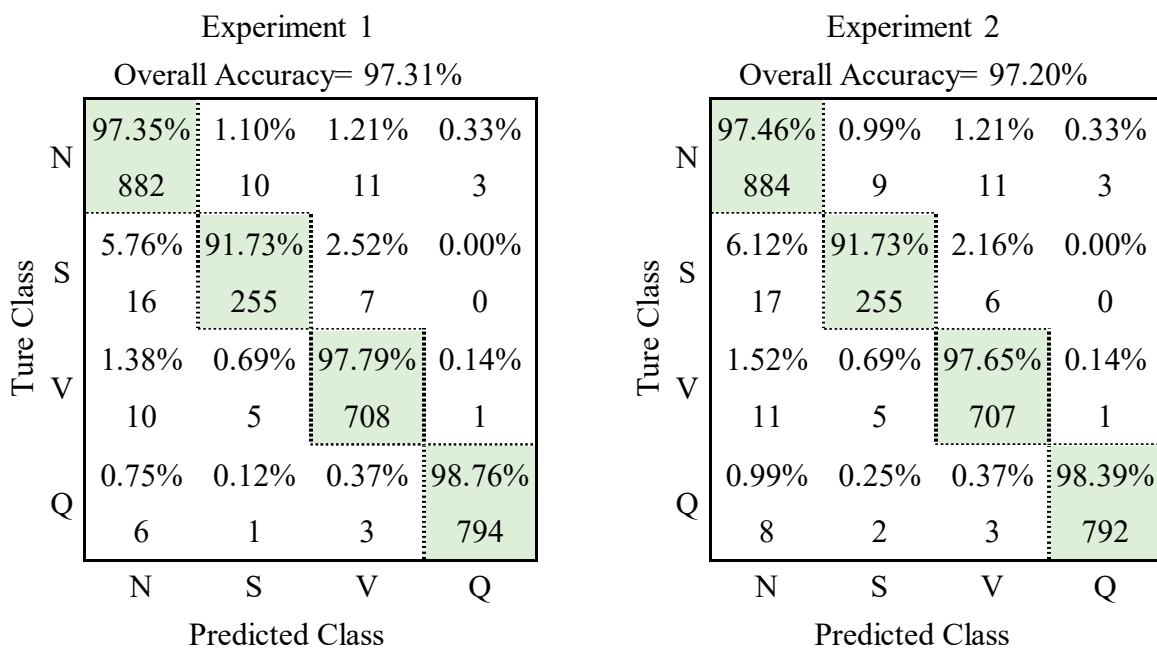


Figure 7. Experiment 1 and Experiment 2 confusion matrices of the heartbeat classification results without F.

3.3. Comparison of Optimizers

This study used the stochastic gradient descent (SGD) optimization method in Experiments 1 and 2 in Section 3.2. In addition, this study used different optimizers, including SGD, adaptive moment estimation (Adam), and root-mean-square propagation (RMSProp), to compare the classification accuracies of different optimizers. In these three optimizers, the learning rate (η) was set to 0.001. Table 7. Performance of the proposed CNN with different optimization methods shows the results of using different optimizers to train the CNN. For both Experiments 1 and 2, SGD achieved the highest accuracy among the methods at 96.47% and 96.79%, respectively. Figures 8 and 9 present the validation loss of Experiments

1 and 2 during convergence of each of these three optimization methods, respectively. The convergence of RMSProp was not satisfactory, having still not converged after 20 epochs.

Table 7. Performance of the proposed CNN with different optimization methods.

Optimization	SGD	Adam	RMSProp
Learning rate (η)	0.001	0.001	0.001
Experiment 1 Acc.	96.47%	95.17%	92.37%
Experiment 2 Acc.	96.79%	93.02%	94.81%

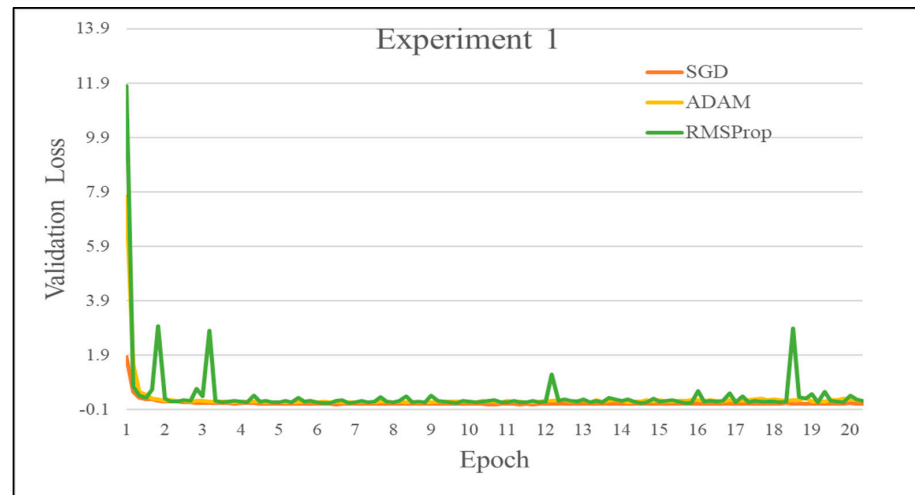


Figure 8. Experiment 1 compares the convergence speeds of three optimizations.

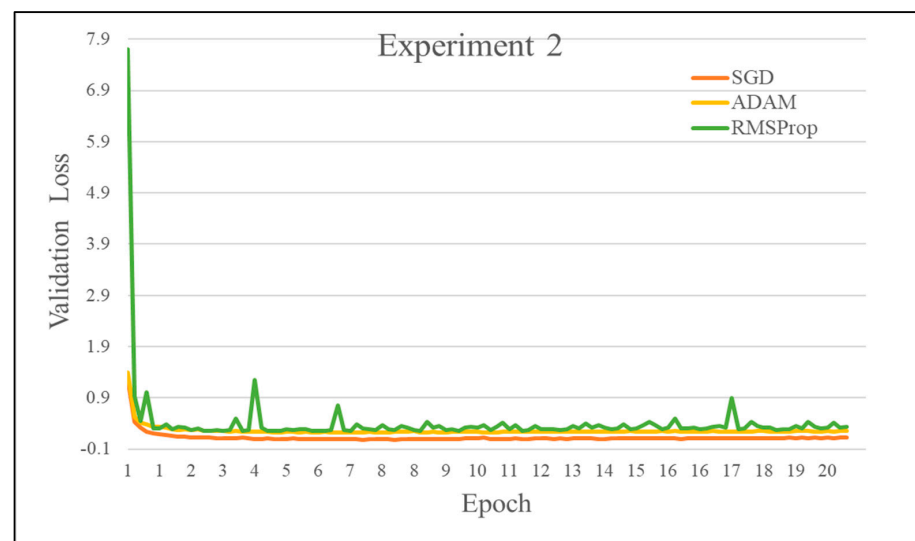


Figure 9. Experiment 2 compares the convergence speeds of three optimizations.

4. Discussion

Many ECG studies have used the MIT-BIH Arrhythmia Database for testing. Table 8 summarizes related research on arrhythmia. Martis et al. [26] and Pławiak [30] have used machine learning methods to extract and classify ECG signal features. Since 2016, scholars have used 1D CNNs for analyzing ECGs because they do not require feature extraction for classification. The subtle changes in ECG signals are hardly detected by the naked eye. Several computer-aided diagnosis systems have been presented in the last decade. The standard steps in conventional machine learning methods for ECG classification are

signal pre-processing, heartbeat segmentation, feature detection, feature selection, and classification. To have higher classification accuracy, different pre-processing methods, feature reduction methods, or extracted features were commonly executed with some human intervention. The more human intervention, the more misjudgment. One of the advantages of CNN is that the steps of feature reduction, feature extraction, and feature selection are no longer required. To minimize the variation and effect of human intervention and to learn the hidden information in the data, CNN is employed in this study. From the literature, the classification accuracies of 1D-CNN (90–99%) [19,21,46,47] are comparable to the results from conventional machine learning methods (90–99%) [26,30]. Instead of a 1D CNN, as in much of the previous literature, a CNN was used to classify ECG images in this study. Moreover, this study used variable signal lengths (Section 2.2.2). Oh et al. [21] used variable signal lengths, too. In Oh’s study, 1D CNN with LSTM was able to achieve 98.10% accuracy for classifying normal sinus rhythm, left bundle branch block (LBBB), right bundle branch block (RBBB), atrial premature beats (APB), and premature ventricular contraction (PVC). Unlike Oh’s study, all fifteen types (five classes) in the MIT-BIH Arrhythmia Database [60] were included in this study.

Table 8. Comparison with related literature.

Year	Author	Length of Signal	No of Classes	Feature Set	Classifier	Overall ACC.
2013	Martis et al. [26]	200 samples	5	DWT+ICA	PNN	99.28%
2016	Zubair et al. [46]	1000 samples	5	Raw data	1D-CNN	92.70%
2017	Acharya et al. [47]	360 samples (1 s)	5	Raw data	1D-CNN	94.03%
2017	Acharya et al. [47]	2 s 5 s	4	Raw data	1D-CNN	92.50% 94.90%
2018	Oh et al. [21]	Variable length	5 *	Raw data	CNN-LSTM	98.10%
2018	Plawiak [30]	3600 samples (10 s)	13 15 17	Frequency components of the power spectral density of the ECG signal	Evolutionary-Neural System (based on SVM)	94.60% 91.28% 90.20%
2018	Yildirim et al. [19]	3600 samples (10 s)	13 15 17	Rescaling raw data	1D-CNN	95.20% 92.51% 91.33%
2018	Yildirim [66]	360 samples	5	Raw data	DBLSTM-WS	99.39%
2019	Jiang et al. [56]	49,953	4	Augmented	DAE+1D-CNN	98.40%
2021	Pal et al. [57]		29	Augmented	CardioNet	98.92%
2021	Ullah [58]	109,446	5 *	Generating new data	CNN	99.12%
2022	Alqudah [67]	10,502 beats	6		MobileNet	93.80%
2022	Ma [59]		5 *	Expanded data	ECG-DCCGAN	98.70%
2023	Pandy et al. [68]		5 *	Balancing data	Hybrid	99.40%
2023	This study	300 samples	5	Raw data	Taguchi+CNN	Experiment 2 96.79%

* Five classes selected from the dataset are not the same as those we selected in the study.

5. Conclusions

This study combines the Taguchi method and CNNs for classifying ECG images from single heartbeats without feature extraction or signal conversion for fifteen heartbeats (five classes) in the MIT-BIH Arrhythmia Dataset. The classification accuracy was 96.79%. The developed system can serve as a starting point for creating a full-fledged tool for the early detection of problems in the ECG signals of patients to guide doctors in their treatment.

The advantages of the proposed models include: classification made by the proposed model that is reproducible with no observer biases; artificial feature extraction and selection that are not required in the proposed model; and the CNN parameter setting that uses the Taguchi orthogonal array and dramatically reduces the number of experiments. There are some drawbacks and limitations; for example, the identification of the R peak is required; small sample sizes for each group are used in this study; the sample size for each group is imbalanced; and each sample cannot simultaneously be a member of multiple classes.

Although the Taguchi-CNN model automatically recognizes five classes of heartbeat on the MIT-BIH Arrhythmia Database with favorable results, the application of similar CNNs on other databases is encouraged and needs to be considered in future research. Since the Taguchi method was applied to reduce the number of experiments, not all parameter combinations were tested in this study. The parameter settings outside the range of this study were not tested. The selected parameter combination with the highest accuracy is only guaranteed within the variable ranges in this study. Other optimization methods for parameter setting are encouraged in future studies. In addition, since a small and imbalanced sample size was used in this study, a larger and more balanced sample size is expected to be tested in the future.

Author Contributions: Conceptualization, M.-L.H. and S.-F.L.; data curation, M.-L.H. and Y.-S.W.; software, Y.-S.W.; formal analysis, M.-L.H. and Y.-S.W.; writing—original draft preparation, M.-L.H. and Y.-S.W.; writing—review and editing, M.-L.H.; supervision, M.-L.H. and S.-F.L. All authors have read and agreed to the published version of the manuscript.

Funding: This research was funded by Ministry of Science and Technology of Taiwan, R.O.C. grant number MOST 108-2221-E-167-001 and MOST 111-2221-E-167-007-MY3. And The APC was funded by Ministry of Science and Technology of Taiwan, R.O.C.

Data Availability Statement: The collected data used in this study are available from the MIT-BIH Arrhythmia Database.

Acknowledgments: The authors gratefully acknowledge the financial support of the Ministry of Science and Technology of Taiwan, R.O.C., through its grants MOST 108-2221-E-167-001 and MOST 111-2221-E-167-007-MY3.

Conflicts of Interest: All authors disclose that they have no financial or personal relationships with any people or organizations that may inappropriately influence (bias) this work.

References

1. Andersen, R.S.; Peimankar, A.; Puthusserypady, S. A deep learning approach for real-time detection of atrial fibrillation. *Expert Syst. Appl.* **2019**, *115*, 465–473. [[CrossRef](#)]
2. Schmidhuber, J. Deep learning in neural networks: An overview. *Neural Netw.* **2015**, *61*, 85–117. [[CrossRef](#)]
3. Hinton, G.E.; Osindero, S.; Teh, Y.-W. A Fast Learning Algorithm for Deep Belief Nets. *Neural Comput.* **2006**, *18*, 1527–1554. [[CrossRef](#)]
4. Krizhevsky, A.; Sutskever, I.; Hinton, G.E. ImageNet classification with deep convolutional neural networks. *Commun. ACM* **2017**, *60*, 84–90. [[CrossRef](#)]
5. Zeiler, M.D.; Fergus, R. Visualizing and Understanding Convolutional Networks. *arXiv* **2013**, arXiv:1311.2901.
6. Hou, J.; Wang, S.; Lai, Y.; Tsao, Y.; Chang, H.; Wang, H. Audio-Visual Speech Enhancement Using Multimodal Deep Convolutional Neural Networks. *IEEE Trans. Emerg. Top. Comput. Intell.* **2018**, *2*, 117–128. [[CrossRef](#)]
7. Al-Antari, M.A.; Al-Masni, M.A.; Choi, M.T.; Han, S.M.; Kim, T.S. A fully integrated computer-aided diagnosis system for digital X-ray mammograms via deep learning detection, segmentation, and classification. *Int. J. Med. Inform.* **2018**, *117*, 44–54. [[CrossRef](#)]
8. Xia, Y.; Wulan, N.; Wang, K.; Zhang, H. Detecting atrial fibrillation by deep convolutional neural networks. *Comput. Biol. Med.* **2018**, *93*, 84–92. [[CrossRef](#)]
9. Al Rahhal, M.M.; Bazi, Y.; Al Zuair, M.; Othman, E.; Benjdira, B. Convolutional Neural Networks for Electrocardiogram Classification. *J. Med. Biol. Eng.* **2018**, *38*, 1014–1025. [[CrossRef](#)]
10. Xu, X.; Wei, S.; Ma, C.; Luo, K.; Zhang, L.; Liu, C. Atrial Fibrillation Beat Identification Using the Combination of Modified Frequency Slice Wavelet Transform and Convolutional Neural Networks. *J. Healthc. Eng.* **2018**, *2018*, 2102918. [[CrossRef](#)]
11. Wang, K.; Kumar, A. Cross-spectral iris recognition using CNN and supervised discrete hashing. *Pattern Recognit.* **2019**, *86*, 85–98. [[CrossRef](#)]
12. Cao, Q.; Lin, L.; Shi, Y.; Liang, X.; Li, G. Attention-Aware Face Hallucination via Deep Reinforcement Learning. *arXiv* **2017**, arXiv:1708.03132.
13. Anthimopoulos, M.; Christodoulidis, S.; Ebner, L.; Christe, A.; Mougiakakou, S. Lung Pattern Classification for Interstitial Lung Diseases Using a Deep Convolutional Neural Network. *IEEE Trans. Med. Imaging* **2016**, *35*, 1207–1216. [[CrossRef](#)]
14. Gao, F.; Wu, T.; Li, J.; Zheng, B.; Ruan, L.; Shang, D.; Patel, B. SD-CNN: A shallow-deep CNN for improved breast cancer diagnosis. *Comput. Med. Imaging Graph.* **2018**, *70*, 53–62. [[CrossRef](#)]
15. Ragab, D.A.; Sharkas, M.; Marshall, S.; Ren, J. Breast cancer detection using deep convolutional neural networks and support vector machines. *PeerJ* **2019**, *7*, e6201. [[CrossRef](#)]

16. Sudharshan, P.J.; Petitjean, C.; Spanhol, F.; Oliveira, L.E.; Heutte, L.; Honeine, P. Multiple instance learning for histopathological breast cancer image classification. *Expert Syst. Appl.* **2019**, *117*, 103–111. [[CrossRef](#)]
17. Helwan, A.; El-Fakhri, G.; Sasani, H.; Uzun Ozsahin, D. Deep networks in identifying CT brain hemorrhage. *J. Intell. Fuzzy Syst.* **2018**, *35*, 2215–2228. [[CrossRef](#)]
18. Acharya, U.R.; Fujita, H.; Lih, O.S.; Hagiwara, Y.; Tan, J.H.; Adam, M. Automated detection of arrhythmias using different intervals of tachycardia ECG segments with convolutional neural network. *Inf. Sci.* **2017**, *405*, 81–90. [[CrossRef](#)]
19. Yildirim, O.; Plawiak, P.; Tan, R.S.; Acharya, U.R. Arrhythmia detection using deep convolutional neural network with long duration ECG signals. *Comput. Biol. Med.* **2018**, *102*, 411–420. [[CrossRef](#)]
20. Faust, O.; Shenfield, A.; Kareem, M.; San, T.R.; Fujita, H.; Acharya, U.R. Automated detection of atrial fibrillation using long short-term memory network with RR interval signals. *Comput. Biol. Med.* **2018**, *102*, 327–335. [[CrossRef](#)]
21. Oh, S.L.; Ng, E.Y.K.; Tan, R.S.; Acharya, U.R. Automated diagnosis of arrhythmia using combination of CNN and LSTM techniques with variable length heart beats. *Comput. Biol. Med.* **2018**, *102*, 278–287. [[CrossRef](#)]
22. Zhao, Z.; Zhang, Y.; Deng, Y.; Zhang, X. ECG authentication system design incorporating a convolutional neural network and generalized S-Transformation. *Comput. Biol. Med.* **2018**, *102*, 168–179. [[CrossRef](#)]
23. Lecun, Y.; Bottou, L.; Bengio, Y.; Haffner, P. Gradient-based learning applied to document recognition. *Proc. IEEE* **1998**, *86*, 2278–2324. [[CrossRef](#)]
24. Simonyan, K.; Zisserman, A. Very Deep Convolutional Networks for Large-Scale Image Recognition. *arXiv* **2014**, arXiv:1409.1556.
25. Szegedy, C.; Wei, L.; Yangqing, J.; Sermanet, P.; Reed, S.; Anguelov, D.; Erhan, D.; Vanhoucke, V.; Rabinovich, A. Going deeper with convolutions. *arXiv* **2014**, arXiv:1409.4842.
26. Martis, R.J.; Acharya, U.R.; Min, L.C. ECG beat classification using PCA, LDA, ICA and Discrete Wavelet Transform. *Biomed. Signal Process. Control* **2013**, *8*, 437–448. [[CrossRef](#)]
27. Martis, R.J.; Acharya, U.R.; Adeli, H.; Prasad, H.; Tan, J.H.; Chua, K.C.; Too, C.L.; Yeo, S.W.J.; Tong, L. Computer aided diagnosis of atrial arrhythmia using dimensionality reduction methods on transform domain representation. *Biomed. Signal Process. Control* **2014**, *13*, 295–305. [[CrossRef](#)]
28. Khalaf, A.F.; Owis, M.I.; Yassine, I.A. A novel technique for cardiac arrhythmia classification using spectral correlation and support vector machines. *Expert Syst. Appl.* **2015**, *42*, 8361–8368. [[CrossRef](#)]
29. Jung, W.H.; Lee, S.G. An Arrhythmia Classification Method in Utilizing the Weighted KNN and the Fitness Rule. *Innov. Res. BioMed. Eng.* **2017**, *38*, 138–148. [[CrossRef](#)]
30. Pławiak, P. Novel methodology of cardiac health recognition based on ECG signals and evolutionary-neural system. *Expert Syst. Appl.* **2018**, *92*, 334–349. [[CrossRef](#)]
31. Sharma, R.R.; Kumar, A.; Pachori, R.B.; Acharya, U.R. Accurate automated detection of congestive heart failure using eigenvalue decomposition based features extracted from HRV signals. *Biocybern. Biomed. Eng.* **2019**, *39*, 312–327. [[CrossRef](#)]
32. Bhagyalakshmi, V.; Pujeri, R.V.; Devanagavi, G.D. GB-SVNN: Genetic BAT assisted support vector neural network for arrhythmia classification using ECG signals. *J. King Saud Univ.—Comput. Inf. Sci.* **2018**, *33*, 54–67. [[CrossRef](#)]
33. Khazaei, M.; Raeisi, K.; Goshvarpour, A.; Ahmadzadeh, M. Early detection of sudden cardiac death using nonlinear analysis of heart rate variability. *Biocybern. Biomed. Eng.* **2018**, *38*, 931–940. [[CrossRef](#)]
34. Gutiérrez-Gnecchi, J.A.; Morfin-Magaña, R.; Lorias-Espinoza, D.; Tellez-Anguiano, A.d.C.; Reyes-Archundia, E.; Méndez-Patiño, A.; Castañeda-Miranda, R. DSP-based arrhythmia classification using wavelet transform and probabilistic neural network. *Biomed. Signal Process. Control* **2017**, *32*, 44–56. [[CrossRef](#)]
35. Lee, H.; Shin, S.-Y.; Seo, M.; Nam, G.-B.; Joo, S. Prediction of Ventricular Tachycardia One Hour before Occurrence Using Artificial Neural Networks. *Sci. Rep.* **2016**, *6*, 32390. [[CrossRef](#)]
36. Pławiak, P.; Abdar, M.; Pławiak, J.; Makarenkov, V.; Acharya, U.R. DGHNL: A new deep genetic hierarchical network of learners for prediction of credit scoring. *Inf. Sci.* **2020**, *516*, 401–418. [[CrossRef](#)]
37. Tuncer, T.; Dogan, S.; Pławiak, P.; Rajendra Acharya, U. Automated arrhythmia detection using novel hexadecimal local pattern and multilevel wavelet transform with ECG signals. *Knowl.-Based Syst.* **2019**, *186*, 104923. [[CrossRef](#)]
38. Kandala, R.; Dhuli, R.; Pławiak, P.; Naik, G.; Moeinzadeh, H.; Gargiulo, G.; Suryanarayana, G. Towards Real-Time Heartbeat Classification: Evaluation of Nonlinear Morphological Features and Voting Method. *Sensors* **2019**, *19*, 5079. [[CrossRef](#)]
39. Pławiak, P.; Abdar, M. Novel Methodology for Cardiac Arrhythmias Classification Based on Long-Duration ECG Signal Fragments Analysis. In *Biomedical Signal Processing—Advances in Theory, Algorithms, and Applications*; Springer: Singapore, 2020; pp. 225–272.
40. Pławiak, P.; Abdar, M.; Rajendra Acharya, U. Application of new deep genetic cascade ensemble of SVM classifiers to predict the Australian credit scoring. *Appl. Soft Comput.* **2019**, *84*, 105740. [[CrossRef](#)]
41. Pławiak, P.; Acharya, U.R. Novel deep genetic ensemble of classifiers for arrhythmia detection using ECG signals. *Neural Comput. Appl.* **2020**, *32*, 11137–11161. [[CrossRef](#)]
42. Luz, E.J.; Schwartz, W.R.; Camara-Chavez, G.; Menotti, D. ECG-based heartbeat classification for arrhythmia detection: A survey. *Comput. Methods Programs Biomed.* **2016**, *127*, 144–164. [[CrossRef](#)]
43. Parvaneh, S.; Rubin, J.; Babaeizadeh, S.; Xu-Wilson, M. Cardiac arrhythmia detection using deep learning: A review. *J. Electrocardiol.* **2019**, *57*, S70–S74. [[CrossRef](#)]
44. Hannun, A.Y.; Rajpurkar, P.; Haghpanahi, M.; Tison, G.H.; Bourn, C.; Turakhia, M.P.; Ng, A.Y. Cardiologist-level arrhythmia detection and classification in ambulatory electrocardiograms using a deep neural network. *Nat. Med.* **2019**, *25*, 65–69. [[CrossRef](#)]

45. Guo, L.; Sim, G.; Matuszewski, B. Inter-patient ECG classification with convolutional and recurrent neural networks. *Biocybern. Biomed. Eng.* **2019**, *39*, 868–879. [CrossRef]
46. Zubair, M.; Kim, J.; Yoon, C. An Automated ECG Beat Classification System Using Convolutional Neural Networks. In Proceedings of the 2016 6th International Conference on IT Convergence and Security (ICITCS), Prague, Czech Republic, 26–29 September 2016.
47. Acharya, U.R.; Oh, S.L.; Hagiwara, Y.; Tan, J.H.; Adam, M.; Gertych, A.; Tan, R.S. A deep convolutional neural network model to classify heartbeats. *Comput. Biol. Med.* **2017**, *89*, 389–396. [CrossRef]
48. Sannino, G.; De Pietro, G. A deep learning approach for ECG-based heartbeat classification for arrhythmia detection. *Future Gener. Comput. Syst.* **2018**, *86*, 446–455. [CrossRef]
49. Li, Z.; Zhou, D.; Wan, L.; Li, J.; Mou, W. Heartbeat classification using deep residual convolutional neural network from 2-lead electrocardiogram. *J. Electrocardiol.* **2020**, *58*, 105–112. [CrossRef]
50. Xiao, Q.; Lee, K.; Mokhtar, S.A.; Ismail, I.; Pauzi, A.L.b.M.; Zhang, Q.; Lim, P.Y. Deep Learning-Based ECG Arrhythmia Classification: A Systematic Review. *Appl. Sci.* **2023**, *13*, 4964. [CrossRef]
51. Samiee, K.; Kiranyaz, S.; Gabbouj, M.; Saramäki, T. Long-term epileptic EEG classification via 2D mapping and textural features. *J. Expert Syst. Appl.* **2015**, *42*, 7175–7185. [CrossRef]
52. Uddin, J.; Nguyen, D.; Kim, J. Accelerating 2D Fault Diagnosis of an Induction Motor using a Graphics Processing Unit. *Int. J. Multimed. Ubiquitous Eng.* **2015**, *10*, 341–352. [CrossRef]
53. Islam, D.M.D.R.; Uddin, J.; Kim, J. Texture analysis based feature extraction using Gabor filter and SVD for reliable fault diagnosis of an induction motor. *Int. J. Inf. Technol. Manag.* **2018**, *17*, 20–32. [CrossRef]
54. Azad, M.; Khaled, F.; Pavel, M. A Novel Approach to classify and convert 1d signal to 2d grayscale image implementing support vector machine and empirical mode decomposition algorithm. *Int. J. Adv. Res.* **2019**, *7*, 328–335. [CrossRef]
55. Li, J.; Si, Y.; Xu, T.; Jiang, S. Deep Convolutional Neural Network Based ECG Classification System Using Information Fusion and One-Hot Encoding Techniques. *Math. Probl. Eng.* **2018**, *2018*, 7354081. [CrossRef]
56. Jiang, J.; Zhang, H.; Pi, D.; Dai, C. A novel multi-module neural network system for imbalanced heartbeats classification. *Expert Syst. Appl.* **2019**, *1*, 100003. [CrossRef]
57. Pal, A.; Srivastava, R.; Singh, Y.N. CardioNet: An efficient ECG arrhythmia classification system using transfer learning. *Big Data Res.* **2021**, *26*, 100271. [CrossRef]
58. Rawi, A.A.; Elbashir, M.K.; Ahmed, A.M. ECG heartbeat classification using CONVXGB model. *Electronics* **2022**, *11*, 2280. [CrossRef]
59. Ma, S.; Cui, J.; Chen, C.L.; Chen, X.; Ma, Y. An effective data enhancement method for classification of ECG arrhythmia. *Measurement* **2022**, *203*, 111978. [CrossRef]
60. MIT-BIH Arrhythmia Database. Available online: <https://archive.physionet.org/physiobank/database/> (accessed on 10 July 2019).
61. ANSI/AAMI EC57; Testing and Reporting Performance Results of Cardiac Rhythm and ST Segment Measurement Algorithms. AAMI Recommended Practice/American National Standard: New York, NY, USA, 1998.
62. Singh, B.N.; Tiwari, A.K. Optimal selection of wavelet basis function applied to ECG signal denoising. *Digit. Signal Process.* **2006**, *16*, 275–287. [CrossRef]
63. Huang, M.L.; Wu, Y.S. Classification of Atrial Fibrillation and Normal Sinus Rhythm based on Convolutional Neural Network. *Biomed. Eng. Lett.* **2020**, *10*, 183–193. [CrossRef]
64. Wan, L.; Zeiler, M.; Zhang, S.; LeCun, Y.; Fergus, R. Regularization of neural networks using dropconnect. In Proceedings of the 30th International Conference on International Conference on Machine Learning, JMLR.org, Atlanta, GA, USA, 17–19 June 2013; Volume 8.
65. Chollet, F. *Deep Learning with Python*; Manning Publications Company: Shelter Island, NY, USA, 2017.
66. Yildirim, Ö. A novel wavelet sequence based on deep bidirectional LSTM network model for ECG signal classification. *Comput. Biol. Med.* **2018**, *96*, 189–202. [CrossRef]
67. Alqudah, A.M.; Qazan, S.; Al-Ebbini, L.; Alquran, H.; Qasmieh, I.A. ECG heartbeat arrhythmias classification: A comparison study between different types of spectrum representation and convolutional neural networks architectures. *J. Ambient. Intell. Hum. Comput.* **2022**, *13*, 4877–4907. [CrossRef]
68. Pandey, S.K.; Shukla, A.; Bhatia, S.; Gadekallu, T.R.; Kumar, A.; Mashat, A.; Shah, M.A.; Janghel, R.R. Detection of Arrhythmia Heartbeats from ECG Signal Using Wavelet Transform-Based CNN Model. *Int. J. Comput. Intell. Syst.* **2023**, *16*, 80. [CrossRef]

Disclaimer/Publisher’s Note: The statements, opinions and data contained in all publications are solely those of the individual author(s) and contributor(s) and not of MDPI and/or the editor(s). MDPI and/or the editor(s) disclaim responsibility for any injury to people or property resulting from any ideas, methods, instructions or products referred to in the content.